Event-chain Monte Carlo and the true self-avoiding walk

A. C. Maggs

CNRS UMR 7083, ESPCI Paris, université PSL, 10 rue Vauquelin, 75005 Paris, France.

E-mail: anthony.maggs@espci.fr

Abstract. We study the large-scale dynamics of event chain Monte Carlo algorithms in one dimension, and their relation to the true self-avoiding walk. In particular, we study the influence of stress, and different forms of interaction on the equilibration and sampling properties of algorithms with global balance, but no local balance.

Introduction

Irreversible Monte Carlo algorithms which rely on global balance [1, 2], while not obeying the more restrictive criterion of detailed balance have had remarkable successes in the study of hard numerical problems such as the nature of ordered phases of two-dimensional fluids [3]. A fundamental question is the origin of the speed-ups compared to classical algorithms, such as molecular dynamics and reversible Monte Carlo [4]. It is clear that such irreversible algorithms are rather unusual for dynamical systems sampling the equilibrium Boltzmann distribution. They display large-scale coherent flows, in a manner that recalls active matter. The collision rules are however finely tuned so that these flows do not disturb the equilibrium state. Indeed, it is because of these large-scale flows that irreversible methods can explore configuration space more efficiently than diffusive algorithms such as Monte Carlo.

In a recent paper [5] we have demonstrated numerically that event-chain Monte Carlo (ECMC) simulation algorithms applied to a harmonic chain are a realization of the so-called "true" self-avoiding walk [6, 7, 8]. Remarkably the true-self avoiding walk has been studied by the mathematical community and solved analytically in one-dimension [9, 10, 11], opening the possibility of better understanding the large-scale dynamic behaviour of irreversible algorithms. The detailed numerical comparisons that we made considered only a harmonic chain in order to remain as close to the exact mathematical results as possible. In this paper we consider a larger range of physical systems and potentials, in order to study the universality of the findings.

The mathematical literature on the true self-avoiding walk emphasizes the importance of two distribution functions. The first $\rho_1(t, x)$ describes the distribution of end-to-end separations, x, in a polymer growth problem. When studying irreversible Monte Carlo methods x maps onto the final position (or rather the label) of the mobile particle at the end of a simulation in which the total displacement of all particles is equal to t. The second distribution $\rho_2(t, h)$ gives the distribution in the number of

previous visits, h to a position for the polymer problem. In the context of Monte Carlo simulation it corresponds the distribution in the number of updates to a particle. For the growing polymer, it was demonstrated that in the one-dimensional continuum limit,

$$\rho_1(t,x) = t^{-2/3}\nu_1(|x|t^{-2/3}) \tag{1}$$
$$\rho_2(t,h) = t^{-1/3}\nu_2(ht^{-1/3}) \tag{2}$$

where the scaling functions ν_1 and ν_2 are known explicitly [10]. They are plotted as solid, red lines in Fig. 7. These scaling functions were confirmed to apply to the ECMC simulation of tension-free harmonic chain. However, in the applications of ECMC with non-trivial potentials this scaling form can not appear: Eq. (1) is symmetric under $x \to -x$, so that the distribution does not drift with time. In ECMC the position of the mobile (active) particle drifts with a constant speed [2], equal to the thermodynamic pressure, so that $\rho_1(t,x)$ can not remain symmetric around the origin, $x = 0$.

The drift, linked to the pressure, can be cancelled by modifying the microscopic interactions on a chain with the addition of an extra linear potential (factor field) [12]. This modified potential is built in such a way that it does not change the thermodynamic properties of the simulated system, only the dynamics through the ECMC update rules. We thus modify the potential between two particles so that

$$V(r) \to V(r) + p\, r \tag{3}$$

Remarkably this modification was found to give rise to further acceleration in the sampling of the underlying physical system. For the optimal choice of the amplitude of the linear potential (factor field) the dynamic exponent z, describing the relaxation of long-wavelength density fluctuations, takes on the low value of $z = 1/2$, rather than the exponents $z = 1$ and $z = 2$ characteristic of molecular dynamics and Monte Carlo methods, and the value $z = 1$ characteristic of the historic ECMC method [12]. This acceleration is directly linked to the exponent $2/3$, appearing in eq. (1). Indeed, the super-diffusive propagation displayed in eq. (1): $|x| \sim t^{2/3}$ is just linked via scaling to the dynamic exponent: $t \sim |x|^{(1+z)}$. Let us also note that a lifted TASEP [13] (Totally Asymmetric Simple Exclusion Process), is believed to have similar scaling properties to ECMC with factor fields and can be studied with the help of Bethe methods. We concluded that there exists a dynamic universality class [5] for one-dimensional systems which is distinct from that which has been widely studied for the KPZ system [14].

The question explored in the present paper is the degree to which this universality class is stable to perturbations in the dynamics coming from modifications in the properties of the underlying physical system. We consider interactions which are more complicated than the harmonic springs of [5], but also a broader range of simulation protocols, such as hot and cold starts as well as quenches in order to see how stable the observed behaviour is. We also study the effect of stress in modifying the distribution of eq. (1).

Implementation of irreversible algorithms

For the implementation of the event chain Monte Carlo we follow the presentation of [15]. The total potential energy of a physical system is broken up into a sum of independent factors. We take as the factors the pair energy of particles in a chain. Motion of a single particle leads to changes in the pair energies, which is then used in

an individualized Monte Carlo criterion (the factorized Metropolis algorithm). This individualized criterion allows one to choose a collision partner among all the changing factors, and to continue the motion with a new mobile particle without generating a Monte Carlo rejection. The unique mobile particle at any moment is called "active". If the pair potential between two particles is $V(r)$ finding the candidate moment of collision, when motion is transferred to a new particle, requires solving an equation of the form

$$\Delta V^+(r) = -T \ln(\text{rand}) \tag{4}$$

rand is uniformly distributed on $(0, 1)$. $T = 1/\beta$ is the temperature. V^+ is constructed from a clipped derivative of V:

$$\frac{dV^+(r)}{dr} = \max\left(0, \frac{dV(r)}{dr}\right) \tag{5}$$

One then compares all the candidate collisions and takes the very first; for a chain with nearest-neighbour interactions this requires the comparison between two candidate events. The implementation is rendered more complicated, because in general we are interested in the addition of an extra linear potential (factor field) [12] to the bare potential $V(r)$, eq. (3).

In this paper we consider three cases. Firstly harmonic chains, where it is possible to find the solution to eq. (4) with elementary functions. Secondly, the case of exponentially repelling particles for which the Lambert-W function [16] allows a direct solution to the energy equation. Finally, Lennard-Jones interacting particles, for which we use iterative root solvers for eq. (4). The Lennard-Jones system is studied at a low temperature where the system breaks into small clusters so that the dynamics is highly heterogeneous.

These different models allow us to explore the universality of the distribution function $\rho_1(t, x)$ as well as test how to implement factor field acceleration in the case that interactions go beyond nearest neighbours. We explore interactions with first and second-nearest neighbours, and show how to implement factor field acceleration in this more general system.

Harmonic chains

We firstly extend our study of the harmonic chain [5]. Our previous work only considered the dynamics of a system prepared in its ground state (cold starts), in a state of zero tension. We firstly study the effects of temperature jumps on the dynamics.

We take as the energy

$$E = \frac{k}{2} \sum_{i=1}^{N} (y_i - y_{i+1})^2 \tag{6}$$

with $y_i \equiv y_{N+i}$. k is a spring constant. The quadratic energy function of a harmonic chain with nearest-neighbour interactions can be written in terms of a sparse (mostly zero-filled) matrix, $E = y^T M y/2$. This matrix M, admits a Cholesky factorization, $M = R^T R$, where R is an upper triangular matrix, again with sparse structure. An equilibrated sample is then found by solving the equation $Ry = \xi$, where y is the configuration and ξ Gaussian distributed, independent random numbers. In order to remove the zero-mode that occurs in M, we attach the last site of the chain to a

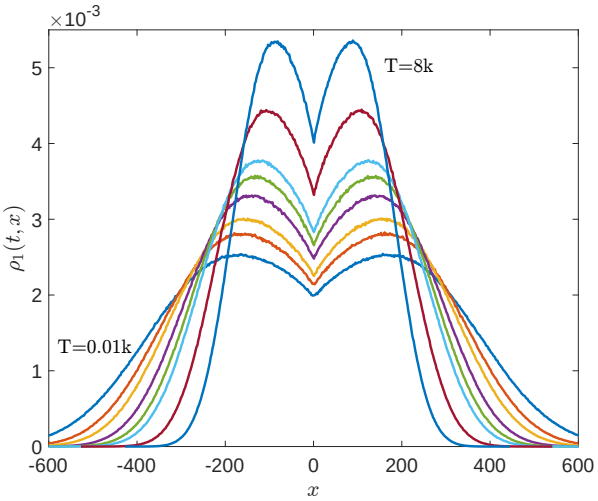

Figure 1. A zero tension harmonic chain is prepared at temperature $T/k = 1$, ECMC simulations are then performed at: $T/k = [0.01, 0.25, 0.5, 1, 1.5, 2, 4, 8]$. Evolution, $\rho_1(t, x)$, eq. (1) for event chain lengths of length $t = 2048$. Higher temperatures spread more slowly giving narrower, higher curves. All curves superpose to within line width on scaling to a standard width. Data from 2^{25} configurations for each curve.

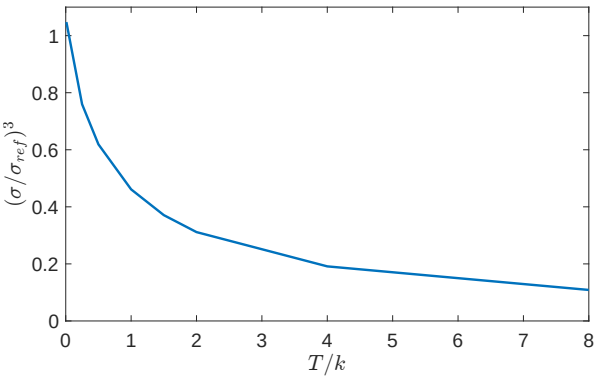

Figure 2. Evolution of the width, σ, of distribution $\rho_1(t, x)$, eq. (1) from the data in Fig. 1. We normalized to width, σ_{ref} in a system prepared at zero temperature and then simulated at $T/k = 1$.

reference position, with an extra spring, during the factorization step but not during the ECMC simulation. This procedure allow us to easily generate equilibrated systems, the algorithmic complexity scaling linearly with the system size.

We generate initial configurations equilibrated at $T/k = 1$, then run the algorithm at different temperatures, if the simulation temperature $T/k < 1$, this imposes a quench on the physical system. If $T/k > 1$ it is a sudden heating. We measure the distribution function $\rho_1(t, x)$ after a constant time t (corresponding to the total displacement of particles during a run), and plot the results in Fig. 1. For all changes in temperature the evolution is remarkably similar, the distribution displays the double peak structure familiar from the analytic solution of the true self-avoiding walk eq. (1).

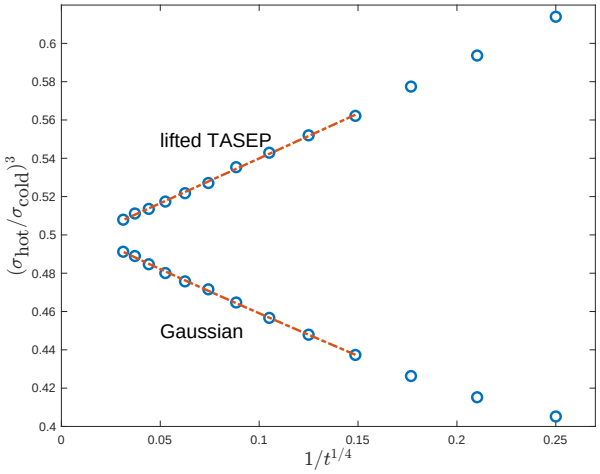

Figure 3. Ratio of widths $\sigma_{\rm hot}$ and $\sigma_{\rm cold}$ for hot and cold starts, as a function of $t^{-1/4}$. The long-time limits extrapolate to $(\sigma_{\rm hot}/\sigma_{\rm cold})^3$ close to 1/2. Times from $t = 2^8$ to $t = 2^{20}$. Red dashed line fit to eq. (7).

When we rescale these curves they superpose to within the displayed line width; the scaling function is insensitive to the surrounding environment. In Fig. 2 we plot the width of the distribution (root-mean-squared deviation), $\sigma^2 = \langle x^2 \rangle$, as a function of the final temperature. In this figure we scale the width by the width of a zero-temperature starting configuration propagating at $T/k = 1$, the protocol that was studied in our previous publication [5]. As temperature increases the distribution narrows.

Exact calculations in [10] on the true-self avoiding walk indicate that if we compare the propagation of a cold start, and a hot start the ratio of widths $(\sigma_{\rm hot}/\sigma_{\rm cold})^3 = 1/2$ This corresponds to the point $(1, 1/2)$ in Fig. 2. In Fig. 3 we study $(\sigma_{\rm hot}/\sigma_{\rm cold})^3$ as a function of simulation time t in order to better evaluate the infinite time limit of the ratio. Empirically we find a near-linear extrapolation if we plot the data as a function of $1/t^{1/4}$. We performed a non-linear fit of our data for large t to the form

$$(\sigma_{\rm hot}/\sigma_{\rm cold})^3 = \alpha_1 + \frac{\alpha_2}{t^{\alpha_3}} \tag{7}$$

using the Matlab function "nlinfit". The result is shown as a dashed line in the Fig 3. We find $(\alpha_1, \alpha_2, \alpha_3) = (0.507, -0.414, 0.233)$. This very slow extrapolation with time prevents us from finding a high precision result, but the results for this ratio for ECMC do seem compatible with the mathematical result for the true self-avoiding walk.

We performed analogous simulations for the lifted TASEP at half filling. We compare starting configurations of either an ordered state ("cold" start) or configurations drawn from the equilibrium distribution ("hot" start). The data displays a very similar scaling as a function of simulation time giving, $(\alpha_1, \alpha_2, \alpha_3) = (0.493, 0.470, 0.251)$

Both extrapolations are rather remarkable, since the microscopic formulation of ECMC on harmonic chains, or lifted TASEP is rather different from the formulation of the true self-avoiding walk. We conclude that there is universality in scaling ratios for ECMC, as well as the scaling function itself.

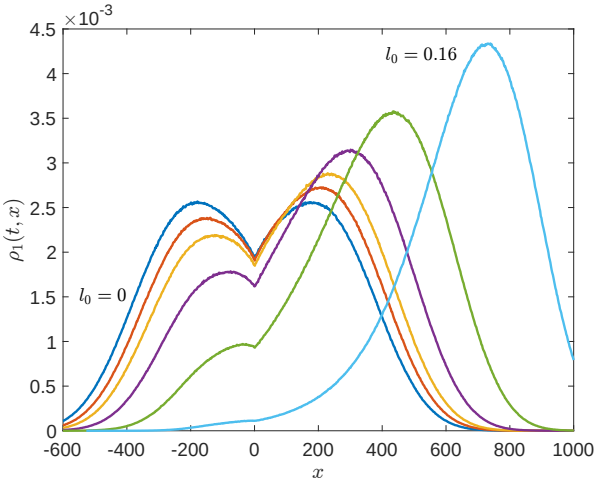

Figure 4. Evolution of distribution, $\rho_1(t,x)$, eq. (1) with stress eq. (8) $l_0 = [0, 0.01, 0.02, 0.04, 0.08, 0.16]$. $N = 8192$, path length $t = 2048$. $T/k = 1$. Data from 2^{26} simulation for each curve.

Stress

Let us now consider the simulation of a harmonic system with strain with the energy

$$E = \frac{k}{2} \sum_{i=1}^{N} (y_{i+1} - y_i - l_0)^2 \tag{8}$$

The ground state of this energy is still $y_i = \text{const}$. This corresponds to stressing each individual spring, by a constant value $p = kl_0$. From the results of [2, 12] this must lead to a change in the large scale dynamics of the algorithm since the stress and mean displacement of the active (mobile) particle are linked by $p = \langle x \rangle / t$. The average position of the distribution $\rho_1(t,x)$ thus displaces with increasing l_0

We perform simulations starting with a ground state configuration $y_i = 0$ (cold start). We see Fig. 4 that imposing a stress leads to a drift of the configuration to the right; we checked that the drift speed is proportional to l_0. Rather remarkably, for small to moderate values of l_0 the singularity at the origin in the curve $\rho_1(t,x)$, remains even as the centre of mass of the curve transports to the right.

General potentials

One dimensional statistical mechanics

The statistical mechanics of a system of particles with nearest-neighbour interactions can be solved analytically in the isobaric ensemble [17]. In particular the distribution of particle separations follows the distribution law $e^{-\beta(V(r)+p\,r)}$, where $V(r)$ is the inter-particle potential for separation r, and p the thermodynamic pressure. From this distribution we find the average separation between particles

$$\Delta(p) = \langle r \rangle_p = \frac{\int r\, e^{-\beta(V(r)+p\,r)}\, dr}{\int e^{-\beta(V(r)+p\,r)}\, dr} \tag{9}$$

With this statistical weight we also find the useful relations:

$$\langle r dV/dr \rangle_p + p\Delta(p) = T \tag{10}$$

$$T\rho_c - \langle dV/dr \rangle_p = p \tag{11}$$

Eq. (10) is the usual virial equation [18], that we use to verify the stress state of our chains. In eq. (11) the contact density, $\rho_c = e^{-\beta V(0)}/z_1$, with z_1 the single bond partition function. When the potential diverges at the origin, as is the case for the Lennard-Jones potential, $\rho_c = 0$, and we have an easy, independent measure of the thermodynamic pressure.

In our simulations we use both cold and hot starts. For the cold start we initialize with a uniformly spaced system, where we calculate, by numerical integration of eq. (9), the mean separation as a function of pressure: and place particles uniformly, with a total system length of $L = N\Delta(p)$. We then use the imposed p as the value of the factor field in our simulations.

For the hot start (where a sample is pre-equilibrated) before each simulation we generate a library of 10^8 samples according to the distribution of eq. (9) using Chebyshev interpolation to implement inverse transform sampling [19]. From this library of separations we generate large numbers of initial states needed to calculate the distributions $\rho_1(t, x)$ and $\rho_2(t, x)$ by randomly drawing a series of N values of r from this library. We expect that differences from the isobaric and constant length ensembles are small for the large system sizes that we simulate.

Longer range interactions

There is no closed form expression for the properties of one-dimensional chains with interactions beyond first-nearest neighbour. It is not possible to generate pre-equilibrated samples as above. We can still, however, use the virial theorem to express the pressure in terms of the potential. We specialize to the case of first and second-nearest neighbour interactions. We have:

$$pL = NT + \sum_{i<j} r_{ij} f_{ij} \tag{12}$$

where $r_{ij} = r_i - r_j$, with the nearest image convention and f_{ij} is the force on i from j. Let us now introduce factor fields p_1 and p_2, between first and second-nearest neighbours, so that for instance the nearest neighbour interaction becomes $V_1(r) + p_1 r$. We find from the virial theorem with the modified potentials:

$$(L/N)p = T + \langle r^{(1)} f_1 + r^{(2)} f_2 \rangle - (L/N)(p_1 + 2p_2) \tag{13}$$

where $f_i(r) = -dV_i(r)/dr$, and $r^{(i)}$ the corresponding separation vector. We anticipate that the zero drift criterion for the distribution $\rho_1(t, x)$, then corresponds to $p = p_1 + 2p_2$. While the zero-drift criterion gives a unique criterion for the factor field with nearest neighbour interactions, this is no-longer the case when longer-ranged interactions are present. We explore numerically the dynamics to determine the efficiency of algorithms with different choices of p_1 and p_2. In particular, we make a detailed study with repulsive exponential interactions.

We generalize the result of eq. (11) using the methods of [20]. We consider a chain of N particles with first and second-nearest neighbour interactions V_1, V_2. We then shorten the chain by ϵ. Clearly $\beta p = -\partial \ln Z/\partial \epsilon$. We implement this shortening by removing a slice in configuration space between 0 and ϵ. We hold a single $i = 1$

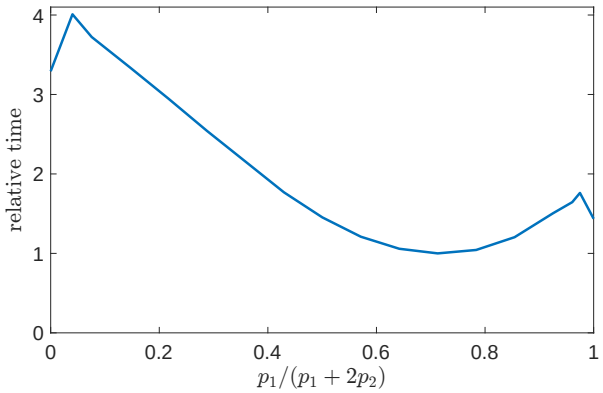

Figure 5. Autocorrelation times of chain with first and second-nearest neighbour exponential potentials, on the line $p = p_1 + 2p_2$. Simulation time, $t = 2^{29}$, $N = 8096$.

particle at $r = 0$, to fix the centre of mass of the chain. Then, for instance the integral over the particle $i = 2$ becomes,

$$\int_{\epsilon}^{r_3} dr_2 \, \exp\left(-\beta V(r_2 - r_1 - \epsilon)\right)$$

With a similar modification for the interaction with the second-nearest neighbours. Keeping variations to order ϵ we find

$$p = T\rho_c - \left\langle \frac{\partial V_1}{\partial r} \right\rangle - 2\left\langle \frac{\partial V_2}{\partial r} \right\rangle$$

The factor of two is due to the fact that shortening a single nearest neighbour separation modifies the distance between two particles at second-nearest neighbour. The erm in ρ_c comes from the disappearance of configurations at contact between the particles $i = 1$ and $i = 2$.

Exponential interactions

We consider the case of repulsive interactions between particles of the form $V(r) = a\exp(-|r|/\ell)$ and systems with first and second neighbour interactions. To implement the event-chain algorithm, with a factor field we need to find the solution, r, to the equation

$$a\exp(-r/\ell) + pr = \Delta E \tag{14}$$

ΔE, is calculated from the difference between V and V^+, together with the thermal activation. Solutions to eq. (14) are found from the Lambert-W function [21], defined as solutions to the equation

$$We^W = z \tag{15}$$

We study two questions with this interaction, firstly the universality of the functions $\rho_1(t, x)$ and $\rho_2(t, x)$ when non-longer working with harmonic springs and secondly how the factor-field method generalizes to systems with longer-range interactions. Let us emphasize that the factor-field method, as previously studied, introduces a linear potential between nearest-neighbour interacting particles, with an

Figure 6. Equilibrated Lennard-Jones configuration at a low density, showing well separated clusters. $\beta\epsilon = 2$, $\beta p = 0.03$, $N = 96$ particles, mean separation. $\Delta = 4.007$.

amplitude which is equal to the thermodynamic pressure. It is at this unique point that the method is the most efficient. With more general interactions there is potentially a line of solutions $p_1 + 2p_2 = p$, where p_i is the factor field with the $i'th$ neighbour and p is again the thermodynamic pressure. In order to generate an efficient algorithm are their further constraints on the individual amplitudes p_i?

We implemented the simulations with $a = 20$, for nearest neighbour interactions and $a = 40$, for second-nearest interactions, with $\ell = 2$, $T = 0.3$, $L = 4.69703N$, $N = 8192$. Preliminary simulations without factor fields are used to estimate the thermodynamic pressure from the virial theorem. We equilibrate the system, and then calculate the autocorrelation time of the lowest Fourier mode of the density. We then perform simulations along the line $p_1 + 2p_2 = p$. The dynamics are characterized by the universal scaling forms, eq. (1, 2); this remains true even for the extreme cases $p_1 = 0$ or $p_2 = 0$.

When measured in terms of the Monte Carlo time t (equal to the total displacement of particles) the code efficiency is almost independent of the exact mix between p_1 and p_2, however extreme choices gives rise to small steps before generating a collision event, so that the clock time of a simulation is sensitive to the exact mix of fields. In Fig. 5 we plot a relative clock time (compared to the best mix of fields) as a function of $p_1/(p_1 + 2p_2)$, demonstrating a relatively broad minimum for the autocorrelation time, in units of wall clock time. Note the two end points for $p_1 = 0$, and $p_2 = 0$ deviate from the main curve, since fewer evaluations of the Lambert-W function are required. We conclude that the universal scaling form remains stable with interactions which go beyond nearest neighbour, and that the efficiency of ECMC depends only weakly on the exact field values, if the factor fields are tuned correctly to the thermodynamic pressure.

Lennard-Jones systems at low densities

We implemented factor-field simulation of particles with nearest-neighbour Lennard-Jones interactions. A previous paper [12] reported the properties of this system at high densities, such that the average separation between particles is smaller than the position of the potential minimum. We here study the properties of a system in which $\beta p = 0.03$, $\Delta = 4.007$, and for which $\epsilon\beta = 2$, where ϵ is the well depth. Length units are set by the Lennard-Jones potential which crosses $E = 0$ for unit separation. As seen in Fig. 6 for these parameters the system breaks up into a series of isolated clusters. The ECMC algorithm must equilibrate the internal structure of the clusters, as well as "jump" the activity between clusters. The question is then whether the large scale dynamics of this heterogeneous system still converges to the universal forms of [10, 5], eq. (1, 2)

Implementation of the factor-field algorithm for the Lennard-Jones potential requires solving equations of the form

$$\frac{1}{r^{12}} - \frac{1}{r^6} + pr = \Delta E \tag{16}$$

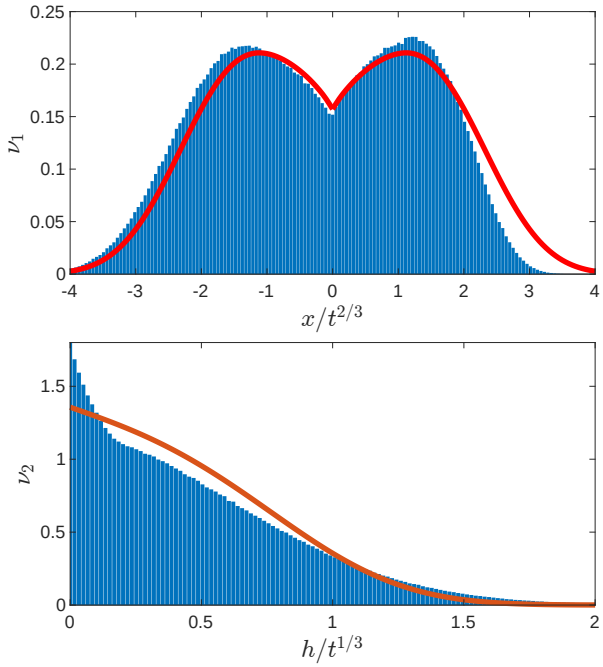

Figure 7. Plots of the scaling functions ν_1 and ν_2, eqs. (1, 2) for a cold start with simulation time $t = 1024$, parameters correspond to Fig. 6. For short times $\rho_1(t, x)$ has a clear back-forwards asymmetry, which only slowly decays for longer simulation times, Fig. 8. $\rho_2(t, h)$ has a pronounced peak for small h. Red, solid lines the analytic solution to the true self-avoiding walk eq. (1, 2) Blue histogram: binned data from simulation.

for r. We proceed by using an iterative solver, based on Halley iteration [21], a higher order generalization of Newton-Raphson. From an initial guess of the root it requires typically four iterations to fully converge the solution of eq. (16) to machine precision.

We find that the "hot", pre-equilibrated samples generate a symmetric function $\rho_1(t, x)$ in agreement with eq (1). However, the cold samples generate a small back-forward asymmetry for $\rho_1(t, x)$, Fig. 7. The distribution of $\rho_2(t, x)$ differs considerably from the analytic form Fig. 7, with a strong peak for small h. This implies that if one stops the simulation one has visited the final visited site much more rarely than would be expected from the statistics of the true self-avoiding walk.

We study the skewness of the distribution $\rho_1(t, x)$, Fig. 8 bottom, as a function of simulation time t, where the skewness is defined as a normalized third moment:

$$\text{skew} = \langle (x - \langle x \rangle)^3 \rangle / \sigma^3 \tag{17}$$

We find that eq. (17) decays only very slowly with t, and possibly at the largest times decays as skew $\sim t^{-1/3}$, which is similar to the asymmetry found in the lifted TASEP model [13]. Despite the slow decay of the skewness of the distribution to zero we find that the width of the distribution, σ, Fig. 8 top, fits the exponent 2/3 from eq. (1) even for short times. Despite showing very slow convergence in time, we conclude that even this heterogeneous system does display the universal true self-avoiding form.

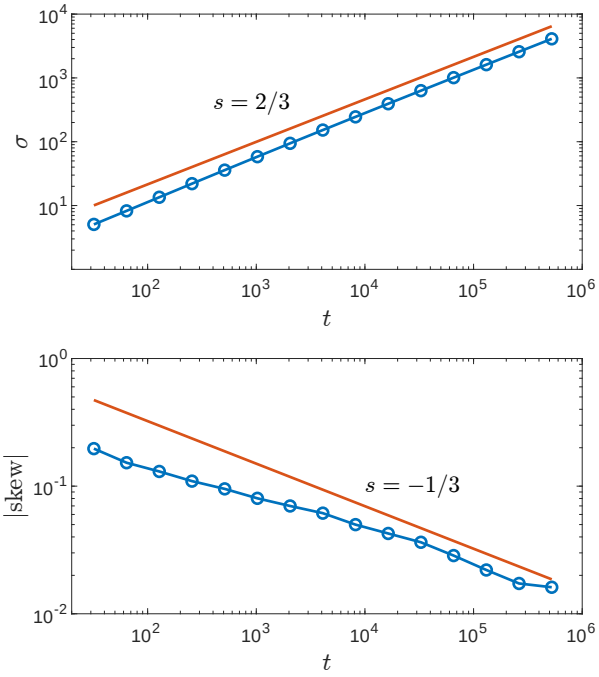

Figure 8. Top: evolution of the width, σ, of the distribution of ρ_1 as a function of simulation time t. Red line as a guide to the eye with exponent $s = 2/3$. Bottom, evolution of the skew with simulation time t. Red line exponent $s = -1/3$ guide to eye. System corresponds to Fig. 6. Data from 2^{22} configurations per point.

Mixing times

Until now, we have used autocorrelation times as a measure of efficiency of a simulation algorithm. However, when starting from an arbitrary configuration one should also have some idea of mixing times, which bound the time for samples generated by the simulation to be close to equilibrium, after starting in an arbitrary state. Certainly in physical applications there are many examples involving nucleation, where this time can be much larger than autocorrelation times. For one-dimensional models with factor-field accelerated ECMC we showed [12] that a system of hard rods, which has an autocorrelation time for density fluctuations scaling as $N^{3/2}$ has an asymptotically slower mixing time scaling as N^2. This is for a configuration where all particles start in contact, and relaxation of the configuration only occurs by loss of particles from the end of a dense starting state. Can one make similar statements for the simulation of models such as the chains considered in this paper? For simplicity, we will only consider configurations of the harmonic chain, to avoid considering configurations such as that displayed in Fig. 6 where the use of very deep Lennard-Jones potentials and very low densities must lead to slow coarsening dynamics.

We proceed by studying trial configurations, that are far from equilibrium, and make analytic arguments which we confirmed with numerical studies. We start with an analogue of the dense configurations which have the largest mixing times for hard rods:

$$y_i = a \qquad 1 \le i \le \lfloor N/2 \rfloor \tag{18}$$

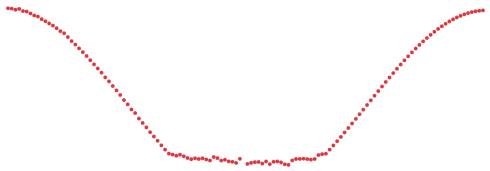

Figure 9. Initial configuration is chosen as eq. (20). The algorithm has driven the active particle to the central part of the configuration, which filled in with a local state which is close to equilibrium. When the ECMC has erased the whole initial state we find a bound on the mixing time.

$$= \quad -a \qquad \text{otherwise}$$

$\lfloor\,\rfloor$ denotes the integer part and $a > 0$ is an amplitude. On starting the position of the active particle at random it will take a time $O(N^{3/2})$ to find the region where $y_i < 0$. For $a^2 k \gg T$ the active particle then remains confined to regions with $y_i < 0$ while making steps of amplitude $O(\sqrt{T/k})$. Thus, it takes a time $O(aN\sqrt{k/T})$ to erase the step in the initial configuration with ECMC. If $a^2 \gg NT/k$ then this time is longer than the autocorrelation time. We can easily build configurations for which the mixing time is unbounded. The case $a^2 = NT/k$ is interesting. It corresponds to injecting energy $O(NT)$ into the chain; comparable to the thermal energy at equilibrium. This motivates two questions.

- (1) Are there configurations with energy $\gg NT$ which nevertheless mix rapidly?
- (2) Are there configurations with an energy budget $O(NT)$ that mix more slowly than eq. (18)?

To answer case (1) we consider the configuration

$$\begin{aligned} y_i &= a \qquad i \text{ odd} \\ y_i &= -a \qquad i \text{ even} \end{aligned} \tag{19}$$

The energy is unbounded for large amplitude a. When the particle activity falls on an "even" site the particle can make a move at once to $y = O(+a)$ and can explore the whole chain in a time $O(N^{3/2})$ independent of the value of a. Thus, there are configurations with arbitrarily high energy with fast mixing.

For case (2) we consider the configuration

$$y_i = N\sqrt{T/k}\cos\left(2\pi i/N\right) \tag{20}$$

The algorithm advances by motion of particles a distance $O(\sqrt{T/k})$, and the energy of this configuration is $O(NT)$. On starting at an arbitrary position the ECMC algorithm runs "downhill" to the smallest values of y_i, Fig. 9, and starts moving the particles with smallest y_i in a positive direction, "filling in" the bottom of the cosine. To erase the initial configuration requires moving each of the N particles a distance $O(N\sqrt{T/k})$. Thus, we have a lower bound on mixing time of N^2, when we require that the energy $O(NT)$ in the initial state, as was found for the hard-rod problem.

Breaking Balance

Given the similarity of ECMC to active matter, with driven trajectories, it is interesting to modify the dynamics in such a way that driven states are no-longer

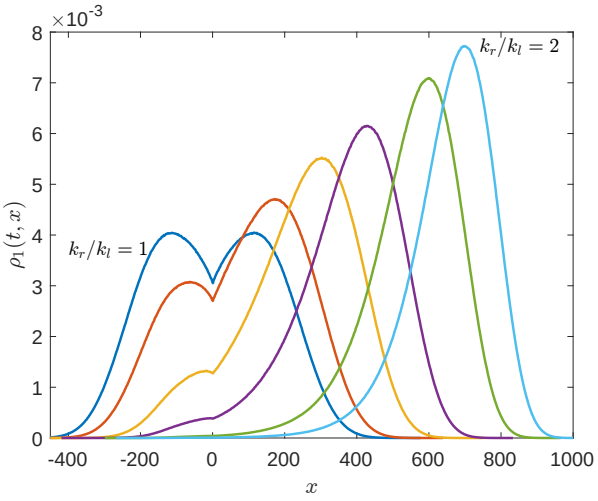

Figure 10. Plots of $\rho_1(t,x)$ for a dynamical system that breaks global balance for ratios $k_r/k_l = [1, 1.1, 1.3, 1.5, 1.8, 2]$, $t = 2048$, $T/k_l = 1$. sargent:Balance/Balance/super2.m

compatible with the Boltzmann distribution. Are the notable features that we recognize for the true self-avoiding walk still present in such a fully non-equilibrium systems. We choose to do this by modifying the interactions in the harmonic chain in such a way that they are non-longer reciprocal [22], that is when the force from i to $i+1$, is different from the force for $i+1$ to i. We modify the form eq. (6) so that in the collision rules eq. (4) different constants k_r and k_l are used for interactions to the right and to the left of the active particle. We perform simulations for several values of k_r/k_l and plot the results in Fig. 10. It is not surprising that distribution $\rho_1(t,x)$ drifts in a manner similar to Fig. 4. However, remarkably the evolution again conserves a singularity at $x = 0$. We have no explanation as to the origin and the stability of this singularity under several forms of perturbation of the true self-avoiding walk.

Conclusions

We have studied variants of the ECMC including factor fields, in order to compare with an exactly soluble model of polymer growth. We find that the distribution functions, which were studied in detail in [5] for a harmonic chain, remain valid even for physical systems that are strongly heterogeneous, such as the Lennard-Jones chain of Fig. 6. Introducing tension however leads to very different distribution functions. It is remarkable however that the singularity at the origin in the function $\rho_1(t,x)$, remains even as the average position drifts. We have no explanation as to why this is so. Similar singularities remain even when breaking global balance.

Acknowledgments

I thank Werner Krauth for extensive discussions on non-reversible simulations and lifted TASEP.

Code

C++ code for simulating the exponential and Lennard-Jones interactions, available from https://github.com/acmaggs/acmaggs.github.io.

References

[1] E. P. Bernard, W. Krauth, and D. B. Wilson, "Event-chain Monte Carlo algorithms for hard-sphere systems," *Phys. Rev. E*, vol. 80, p. 056704, Nov 2009. [Online]. Available: https://link.aps.org/doi/10.1103/PhysRevE.80.056704

[2] M. Michel, S. C. Kapfer, and W. Krauth, "Generalized event-chain Monte Carlo: Constructing rejection-free global-balance algorithms from infinitesimal steps," *The Journal of Chemical Physics*, vol. 140, no. 5, p. 054116, 02 2014. [Online]. Available: https://doi.org/10.1063/1.4863991

[3] E. P. Bernard and W. Krauth, "Two-step melting in two dimensions: First-order liquid-hexatic transition," *Phys. Rev. Lett.*, vol. 107, p. 155704, Oct 2011. [Online]. Available: https://link.aps.org/doi/10.1103/PhysRevLett.107.155704

[4] S. C. Kapfer and W. Krauth, "Irreversible local Markov chains with rapid convergence towards equilibrium," *Phys. Rev. Lett.*, vol. 119, p. 240603, Dec 2017. [Online]. Available: https://link.aps.org/doi/10.1103/PhysRevLett.119.240603

[5] A. C. Maggs, "Non-reversible Monte Carlo: An example of "true" self-repelling motion," *Europhysics Letters*, vol. 147, no. 2, p. 21001, aug 2024. [Online]. Available: https://dx.doi.org/10.1209/0295-5075/ad64ff

[6] D. J. Amit, G. Parisi, and L. Peliti, "Asymptotic behavior of the "true" self-avoiding walk," *Phys. Rev. B*, vol. 27, pp. 1635–1645, Feb 1983. [Online]. Available: https://link.aps.org/doi/10.1103/PhysRevB.27.1635

[7] L. Peliti, "Self-avoiding walks," *Physics Reports*, vol. 103, no. 1, pp. 225–231, 1984. [Online]. Available: https://www.sciencedirect.com/science/article/pii/037015738490084X

[8] R. Rammal, J. C. A. d'Auriac, and A. Benott, "Statistics of the true self-avoiding walk in one dimension," *Journal of Physics A: Mathematical and General*, vol. 17, no. 1, p. L9, jan 1984. [Online]. Available: https://dx.doi.org/10.1088/0305-4470/17/1/003

[9] B. Tóth, "The "True" Self-Avoiding Walk with Bond Repulsion on $\mathbb{Z}$: Limit Theorems," *The Annals of Probability*, vol. 23, no. 4, pp. 1523 – 1556, 1995. [Online]. Available: https://doi.org/10.1214/aop/1176987793

[10] L. Dumaz and B. Tóth, "Marginal densities of the "true" self-repelling motion," *Stochastic Processes and their Applications*, vol. 123, no. 4, pp. 1454–1471, 2013. [Online]. Available: https://www.sciencedirect.com/science/article/pii/S0304414912002517

[11] B. Tóth and W. Werner, "The true self-repelling motion," *Probability Theory and Related Fields*, vol. 111, no. 3, pp. 375–452, 1998. [Online]. Available: https://doi.org/10.1007/s004400050172

[12] Z. Lei, W. Krauth, and A. C. Maggs, "Event-chain Monte Carlo with factor fields," *Phys. Rev. E*, vol. 99, p. 043301, Apr 2019. [Online]. Available: https://link.aps.org/doi/10.1103/PhysRevE.99.043301

[13] F. H. L. Essler and W. Krauth, "Lifted tasep: a Bethe ansatz integrable paradigm for non-reversible Markov chains," 2023. [Online]. Available: https://arxiv.org/abs/2306.13059

[14] M. Kardar, G. Parisi, and Y.-C. Zhang, "Dynamic scaling of growing interfaces," *Phys. Rev. Lett.*, vol. 56, pp. 889–892, Mar 1986. [Online]. Available: https://link.aps.org/doi/10.1103/PhysRevLett.56.889

[15] M. F. Faulkner, L. Qin, A. C. Maggs, and W. Krauth, "All-atom computations with irreversible Markov chains," *The Journal of Chemical Physics*, vol. 149, no. 6, p. 064113, 08 2018. [Online]. Available: https://doi.org/10.1063/1.5036638

[16] R. M. Corless, G. H. Gonnet, D. E. G. Hare, D. J. Jeffrey, and D. E. Knuth, "On the Lambert W function," *Advances in Computational Mathematics*, vol. 5, no. 1, pp. 329–359, 1996. [Online]. Available: https://doi.org/10.1007/BF02124750

[17] R. Feynman, *Statistical mechanics: a set of lectures*, ser. Frontiers in physics : a lecture note and reprint series. Sarat Book Distributors, 1972. [Online]. Available: https://books.google.fr/books?id=Vflsca1UFZoC

[18] A. Maggs, "The virial theorem with periodic boundary conditions," *Chemical Physics Letters*, vol. 816, p. 140389, 2023. [Online]. Available: https://www.sciencedirect.com/science/article/pii/S0009261423000945

[19] T. A. Driscoll, N. Hale, and L. N. Trefethen, *Chebfun Guide*. Pafnuty Publications, 2014. [Online]. Available: http://www.chebfun.org/docs/guide/

[20] B. Li, Y. Nishikawa, P. Höllmer, L. Carillo, A. C. Maggs, and W. Krauth, "Hard-disk pressure computations-a historic perspective," *The Journal of Chemical Physics*, vol. 157, no. 23, p. 234111, 12 2022. [Online]. Available: https://doi.org/10.1063/5.0126437

[21] "Boost C++ libraries," 2024, https://www.boost.org/doc/libs/1_86_0/libs/math/doc/html/root_finding.html.

[22] M. Fruchart, R. Hanai, P. B. Littlewood, and V. Vitelli, "Non-reciprocal phase transitions," *Nature*, vol. 592, no. 7854, pp. 363–369, 2021. [Online]. Available: https://doi.org/10.1038/s41586-021-03375-9